2-1-2016

Selection and Control of Individual Domain Walls in Nanowire Arrays via Asymmetric Depinning Fields

Andrew Kunz
Marquette University, andrew.kunz@marquette.edu

H. Henry Le
Marquette University

Demetrious Kutzke
Marquette University

Jesse Vogeler-Wunsch
Marquette University

Accepted version. *IEEE Transactions on Magnetics,* Vol. 52, No. 2 (February 2016). DOI.

Selection and control of individual domain walls in nanowire arrays via asymmetric depinning fields

Andrew Kunz, H. Henry Le, Demetrious Kutzke, and Jesse Vogeler-Wunsch

Physics Department, Marquette University, Milwaukee, WI 53201, USA

Abstract

Artificially inscribed notches are often used to pin domain walls (DWs) in ferromagnetic nanowires. The process of selecting and moving the trapped DW in nanowire arrays is an important step for potential applications. The chirality of a DW leads to a pair of pinning positions at the inscribed notches which can be modeled by a symmetric double well. The depinning field depends on the side of the well the DW is trapped with respect to the applied field direction and the DWs can also be transitioned between the two wells without depinning. We demonstrate how manipulating the double well improves DW selectivity and control in wire arrays containing multiple DWs.

The motion of a domain wall (DW) through thin, ferromagnetic nanowires is of interest due to a variety of potential applications in magnetic recording, sensing, and logic operations [1 – 5]. A DW is the transition region between two oppositely oriented ferromagnetic domains where the magnetic moments rotate. In a thin nanowire a DW is a robust, topologic feature leading to good stability [6 – 7]. For many of the proposed technologies to be viable it is necessary to select and controllably manipulate a single DW in an array of nanowires where each wire contains multiple DWs. Here we demonstrate how an individual domain wall can be selected and moved in such an array due to an asymmetric depinning process found at notches.

In most applications a DW is driven along the length of a wire either by the application of an applied field, or a current; in both cases every DW in the wire responds and moves to the given stimulus unless trapped. Artificial notches are often inscribed along the edges of the wires to trap and hold DWs in known locations. The pinning strength of the notch is known to depend on its shape, its dimensions, and its location along the wire with respect to the type and chirality of the DW to be trapped [8 – 17]. A variety of techniques have been demonstrated to depin a single domain wall in a single wire, or to move all the domain walls in a wire at once; however, individual control of a single domain wall in an array of wires containing multiple DWs remains an essential step [18 – 21]. In some instances the chirality of the DW leads to an asymmetry in the depinning field because a pair of pinning locations exists at the notch [9, 10]. We explore this asymmetric pinning strength which arises due to the direction of the depinning field with respect to the DW chirality and pinning location. It is worth noting that in the case of current assisted depinning that this asymmetry does not exist as the depinning mechanism is only due to the transfer of momentum from the electrons to the magnetic moments in the DW. However, the field induced asymmetry can be taken advantage of to improve both selectivity and control of an

individual DW in a wire containing multiple DWs by transitioning the DWs across the notch. The technique is easily extended to nanowire arrays by utilizing local fields created by current carrying wires. In order to investigate the depinning behavior we investigate the trapping potential of the notches with micromagnetic simulation [22].

Standard micromagnetic simulation is employed to explore the interaction of a domain wall with a notch located along the edge in the center of the nanowire. We integrate the Landau-Lifshitz equation of motion for the three dimensional rotation of the magnetic moments *m* in the wire

$$\frac{\partial \vec{m}}{dt} = -\gamma\left(\vec{m} \times H\right) - \alpha \vec{m} \times \frac{\partial \vec{m}}{\partial t} \qquad (1)$$

with gyromagnetic ratio γ = 17.6 MHz/Oe. The total magnetic field *H* includes the external field as well as the dipole and exchange fields with materials parameters for permalloy including saturation magnetization M_s = 800 emu/cm^3, and exchange constant A = 1.3 x 10^{-6} erg/cm with no crystalline anisotropy. The interaction between a domain wall and a notch extends over a relatively small distance from the notch therefore we simulate wires with a minimum length of just three microns. In this study each wire had a rectangular cross section of width of 100 nm and thickness 5 nm to ensure transverse domain walls as shown in Fig. 1. Each wire was discretized into identical 5 nm cubes and integrated utilizing a Hamming's method 4th order predictor corrector technique with a simulated integration time step less than a picosecond. The damping parameter is $\alpha = 0.008$. In each trial a symmetric triangular notch is positioned at the center of the wires long axis located along either the top or bottom edge. We employ free boundary conditions along all edges of the wire with a minimum distance of a micron between a notch and the wire's ends to minimize interactions. The results presented here are for a notch

with base of 30 nm and a penetration depth into the wire of 30 nm. (We investigated triangular, rectangular, and circular notches with bases and depths ranging from 20 – 60 nm; the pinning strengths vary across these trials but the results presented are typical.) Because we created triangles from a cubic discretization we investigated the dependence on the discretization size and found no significant difference in the depinning fields. It is expected that there are small quantitative differences between simulated results and those of experiment, or a finite element technique, however the qualitative agreement should be good and within the uncertainty expected from trying to experimentally create a perfect notch.

There are two primary techniques to find the depinning field for a DW trapped at a notch [14 – 17]. There is a dynamic approach where the field is suddenly applied to the trapped DW and a static approach where the field is slowly incremented over time; these two approaches give slightly different results and we use both processes for the reasons given below.

To find the dynamic depinning field a domain wall was the pinned at the notch and relaxed for a long time to ensure an equilibrium starting state. Always starting from this relaxed, zero field, state a magnetic field was applied along the long axis of the wire. If the DW remained trapped at the notch, the trial was restarted from the initial zero field equilibrium state with a stronger field applied. The first field for which the domain wall releases, and propagates away, from the notch is considered the dynamic depinning field. This dynamic approach mirrors what would be used in applications where the applied fields would be quickly turned on and off, or reversed. In the case of transverse fields, the transverse field was first applied to the wire until the DW reached equilibrium at which point the longitudinal field was applied [20].

To explore the energy landscape of the domain wall in the wire the static depinning approach was followed. In this case we started from the equilibrium state but slowly and steadily increased the applied field, in 1 Oe increments, tracking the energy of the domain wall as a function of its position from the center of the notch. The position of the domain wall was calculated by tracking the long axis magnetization of the wire [23]. The center of the DW is given by

$$x_{dw} = \frac{L}{2}\langle m_x \rangle \qquad (2)$$

where L is length of the wire and m_x is the average long axis magnetization (ref). This approach essentially treats the DW like a point object; however the DW is a finite sized object with a narrow structure (roughly 100 nm wide in a 3000 – 5000 nm long wire) that becomes slightly elongated as fields are applied to remove it from the notch. We alternately verified the domain wall location by finding the location where m_x changes sign for each row of data and averaging; the two techniques give equivalent results.

Single notches can be inscribed along either the top or bottom edge of a wire. In Fig. 1 we show the three possible pinning locations for a DW with clockwise chirality when incident on a symmetric triangular notch [10]. In a simple representation, a transverse domain wall consists of a pair of topologic defects with opposite (fractional) winding numbers such that the net topologic charge of the domain wall is zero [6, 7, 24]. For the head to head, clockwise rotation, DW in Fig.1 the negative topologic charge is located along the upper edge, with the positive charge along the bottom. When a negative charge is incident on a triangular notch the DW becomes strongly pinned in the center of the notch. The field necessary to dynamically depin the DW is also shown in Fig. 1. Due to the location of the DW, in the center of the trap, the

depinning field is found to be symmetric with respect to the direction of the applied field. A more interesting case arises when the positive topologic charge is incident on the notch as observed in the bottom pair of images in Fig. 1. The DW can be trapped on either side of the notch. For a symmetric notch there is no preference for the DW to be on either side but the field necessary to depin the DW depends on the direction it is applied [9, 10]. There is a "hard" and "easy" direction with respect to the pinning location and the field direction; it is easy for the DW to depin when it is pushed across the notch (~25 Oe), and hard when pulled away from the notch on the same side (~41 Oe). A key feature, allowing for improved selectivity and control, is the even lower field that can be applied to transition the DW back and forth across the notch; just 16 Oe is needed to dynamically move the DW from one side of the notch to the other. Because this transition field is lower than either depinning field the DW remains trapped but can be placed into the hard or easy position as needed.

A critical aspect for DW motion in nanowires is the strength of the driving field due to the onset of Walker breakdown [25]. For small driving fields a DW moves quickly with a constant magnetic structure (constant chirality). However in larger fields the speed slows and the DW undergoes structural transitions, therefore it is beneficial to use weak fields [25]. Additionally, in a nanowire array the fields will need to be applied locally. These Oersted fields can be created by current carrying wires [26]. It is beneficial to use small fields such that the energy requirements are minimized. In the wires investigated here 25 Oe is above the critical field so even the easy depinning field is too large. A second field, applied in the plane of the wire but perpendicular to the long axis, a transverse field, can be used to vary the depinning field as shown in Fig. 2 [20, 26]. A negative transverse field corresponds to a field aligned parallel to the magnetic moments in the DW, positive is anti-parallel. When the alignment is parallel the

depinning fields drop. Fig. 2B shows that a 50 Oe transverse field is sufficient to lower the easy depinning field below the Walker threshold. Just as importantly, the anti-parallel alignment leads to an increase in the pinning strength. Note that the depinning fields, shown in Fig. 2(a), for the positive topologic charge remain too large even in strong transverse fields.

In Fig. 2(b) we show the dependence of the transition field on the transverse field. Again parallel alignment lowers the transition field; anti-parallel alignment leads to an increase. In the case of parallel alignment there is a greater than 10 Oe difference in the transition field to the easy depinning field which means it should be possible to position the DW to be released or held as necessary. In addition from the simulations we note: the notch is symmetric, there are two identical DW trapping locations, and there is a need for a field to move the DW out of the notch or to move the DW between the two pinning locations. This combination is best described by an energy landscape consisting of a double well. We map the energy landscape of the DW in the wire using the static depinning approach. With the DW trapped on one side of the notch, the field is slowly incremented in 1 Oe steps. At the end of each field step the energy in the wire and the location of the domain wall is recorded. Fig. 3(a) shows the calculated energy landscape as a function of domain wall position. The total energy shown is the total exchange and magnetostatic energy for the wire when the domain wall is at the noted position. We are primarily concerned with how the energy changes with respect to the location of the domain wall around the notch as this is where the energy landscape is noted to vary. We note that there are two symmetrically located wells separated by an energy barrier that is smaller than the sides of the well. The height of the central barrier is roughly $7k_BT$ at room temperature so the pinning locations are thermally stable. The red and blue circles are tools to represent the possible locations of a DW in the potential well. The symmetry of the well is broken by applying an

external field along the wires long axis. The Zeeman energy $U_{Zeeman} = -\vec{M} \cdot \vec{H}_{ext}$ adds a linear term to the interaction energy raising one of the energy minimas with respect to the other, depending on the direction of the applied field. It is worth mentioning that in the case of current assisted DW depinning the landscape doesn't change and equal amounts of momentum (i.e. current) would be necessary to depin the DW in both directions. The simulations show a 16 Oe applied along the *+x* axis is sufficient to transition the DW from the left well to the right well, whereas a DW in the right well would remain trapped. In Fig. 3(b) we represent how the shape of the energy landscape in Fig. 3(a) is varied when a 16 Oe field is applied. Note that there is still a small well on the left side but the sudden onset of the applied field lifts the domain wall above the height of the central barrier (dashed lines) giving the domain wall enough energy to transition across the notch. It should be noted that the presence of the well on the left side highlights the difference between the static and dynamic depinning processes. In the static case the DW always remains near equilibrium and therefore in the well, whereas in the dynamic case the sudden onset of the field gives the DW increased energy to move. The right well is lowered but remains deep enough to trap all DWs. A DW initially in the left well dynamically depins completely from the notch when 25 Oe is applied. Fig. 3(c) shows the energy for this situation. In this case the right well still exists, to the extent than a DW that starts in the right well will remain there. However, the left well has been raised sufficiently that a DW starting in the left well has sufficient kinetic energy when it reaches the location of the right well to escape. In the static case the DW that started in the left well would have transitioned to the right well before the 25 Oe field was applied. In this static case the DW would remain in the right hand well until the field is sufficiently increased. Fig. 3(d) shows the energy landscape when a 41 Oe field is applied. In this case the right well has not quite been removed but a DW in the right well would

be raised above the maximum energy barrier (dashed lines) and all DWs that were trapped in this notch would be released. This series of images demonstrates that the asymmetric depinning fields arise from the existence of double well energy landscape and the asymmetry imposed by the Zeeman energy due to the spatial separation of the two wells.

The asymmetric depinning process is something that can be exploited to select and control an individual domain wall in an array of wires each containing multiple domain walls. Fig. 4 shows a pair of wires each containing three domain walls all of the same chirality trapped by notches (labeled 1 – 5) located along the bottom edge of the wires. The chirality can be set in a variety of ways including preferential injection techniques [27 - 29]. At time t = 0 ns, the DWs in Fig. 4(a) at notches 1 and 5 are aligned head to head while the DWs at notch location 4 are tail to tail. We arbitrarily select the DW in the top wire at notch 1 to be repositioned to notch location 2. A globally applied field would likely move all of the DWs in the image and a local field at notch 1 would also move the DW in the bottom wire. However by applying local fields, such as could be accomplished using MRAM type architecture of crisscrossing current carrying wires, as represented by the cartoon shaped pulses we first transition the top DW across notch 1 (to the easy side) as shown in Fig. 4(b). Next a local pulse, now in the $+x$ direction, is applied at notch 1 in combination with a transverse field pulse in the top wire, to depin the DW and move it to notch location 2, Fig. 4(c). Then a local field is applied at notch location 4 along the $+x$ direction along with a transverse field in the bottom wire to move the DW from notch 4 to notch 3, Fig 4(d). Finally a pulse is applied at notch location 5, with a transverse field in the bottom wire, to transition the DW from location 5 to 4, Fig 4(e) at time t = 24 ns. Note that only the selected DWs leave their pinning locations demonstrating quick and reliable individual selection and control of a given DW in an array of wires using only applied fields. The longitudinal fields

applied were never greater than 20 Oe and the transverse fields were 50 Oe; field strengths that are below the critical Walker field, ensuring that the DW structure remains constant as the DW moves through the wire, and which can be efficiently created.

In summary chiral DWs trapped at notches can be subject to a pair of pinning locations due to the symmetric double well energy landscape. The pinning locations, with respect to the applied field direction, determine the depinning field for the DW. It is possible to transition a DW from one pinning site to the other without completely depinning the DW which makes it possible to take advantage of the asymmetry in depinning fields. We demonstrate selection and controlled movement of trapped ferromagnetic DWs in pair of wires containing multiple DWs using only locally applied fields; a technique not suitable for current assisted DW depinning.

Acknowledgment

This work was supported by the National Science Foundation (DMR 1006947 & 1309094).

References

1. S. S. P. Parkin, M. Hayashi, and L. Thomas, "Magnetic Domain-Wall Racetrack Memory,"Science **320**, pp. 190-194, Apr. 2008.
2. M. T. Bryan, T. Schrefl, and D. A. Allwood, "Symmetric and Asymmetric domain wall diodes in magnetic nanowires," Appl. Phys. Lett. 91, 142502, 2007.
3. D. A. Allwood, G. Xiong, C. C. Faulkner, D. Petit, and R. P. Cowburn, "Magnetic domain-wall logic," Science 309, 1688-1692, Sept. 2005.
4. M. Hayashi, L. Thomas, R. Moriya, C. Rettner, and S. S. P. Parkin, "Current-controlled magnetic domain-wall nanowire shift register," Science 320, 209-211, Apr. 2008.

5. M. Fukadam M. Yamanouchi, F. Matsukura, and H, Ohno, "Switching of tunnel magnetoresistance by domain wall motion in (Gas,Mn)As-based magnetic tunnel junctions, Appl. Phys. Lett. 91, 052503 (2007).
6. O.A. Tretiakov, D. Clarke, G.-W. Chern, Y.B. Bazaliy, and O. Tchernyshyov, "Dynamics of domain walls in magnetic nanostrips," Phys. Rev. Lett. 100, 127204 (2008).
7. A. Kunz, "Field induced domain wall collisions in thin magnetic nanowires," Appl. Phys. Lett. 94, 132502 (2009).
8. D. Petit, A. –V. Jausovec, D. Read, and R. P. Cowburn, "Domain wall pinning and potential landscapes created by constrictions and protrusions in ferromagnetic nanowires," J. Appl. Phys. 103, 114307 (2008).
9. M. Hayashi, L. Thomas, C. Rettner, R. Moriya, X. Jiang, and S. S. P. Parkin, "Dependence of current and field driven depinning of domain walls on their structure and chirality in permalloy nanowires," Phys. Rev. Lett. 97, 207205 (2006).
10. S. Goolaup, S. C. Low, M. C. Sekhar, and W. S. Lew, "Dependence of pinning on domain wall spin structure and notch geometry," J. of Phys: Conf. Series 266, 012079 (2011).
11. L. K. Bogart, D. Atkinson, K. O'Shea, D. McGrouther, S. McVitie, "Dependence of domain wall pinning potential landscapes on domain wall chirality and pinning site geometry in planar nanowires," Phys. Rev. B 79, 054414 (2009).
12. L. K. Bogart, D.S. Eastwood, D. Atkinson, "The effect of geometrical confinement and chirality on domain wall pinning behavior in planar nanowires," J. Appl. Phys 104, 033904 (2008).
13. D. S. Eastwood, J. A. King, L.K. Bogart, H. Cramman, and D. Atkinson, "Chirality-dependent domain wall pinning in a multinotched planar nanowire and chirality preservation using transverse magnetic fields," J. Appl. Phys. 109, 013903 (2011).
14. M.-Y. Im, L. Bocklage, P. Fischer, and G. Meier, "Direct observation of stochastic domain-wall depinning in magnetic nanowires" Phys. Rev. Lett. 102, 147204 (2009).
15. H. Tanigawa, T. Koyama, M. Bartkowiak, S. Kasai, K. Kobayashi, T. Ono, and Y. Nakatani, "Dynamical pinning of a domain wall in a magnetic nanowire induced by Walker breakdown," Phys. Rev. Lett 101, 207203 (2008).

16. S.-M. Ahn, K.-W Moon, D.-H Kim, and S.-B. Choe, "Detection of the static and kinetic pinning of domain walls in ferromagnetic nanowires," Appl. Phys. Lett. 95, 152506 (2009).
17. S.-M. Ahn, K.-W Moon, D.-H Kim, and S.-B. Choe, "Geometric dependence of static and kinetic pinning of domain walls on ferromagnetic nanowires," J. Appl. Phys. 111, 07D309 (2012).
18. A. Zhukov, J. M. Blanco, A. Chizhik, M. Ipatov, H. Rodionova, and V. Zhukova, "Manipulation of domain wall dynamics in amorphous microwires through domain wall collision," J. Appl. Phys. 114, 043910 (2013).
19. A. Himeno, K. Kondo, H. Tanigawa, S. Kasai, and T. Ono, "Domain wall ratchet effect in a magnetic wire with asymmetric notches," J. Appl. Phys. 103, 07E703 (2008).
20. S. Glathe, U. Hubner, R. Mattheis, and P. Seidel, "Influence of transverse fields on domain wall pinning in ferromagnetic nanostripes," J. Appl. Phys. 112, 023911 (2012).
21. J. –S. Kim, et al, "Synchronous precessional motion of multiple domain walls in a ferromagnetic nanowire by perpendicular field pulses," Nature Comm. (5) 3429, March 2014. DOI: 10.1038/ncomms4429.
22. LLG Micromagnetic Simulator v2.63c, M. R. Scheinfein (2009).
23. D. G. Porter, and M. J. Donahue, "Velocity of transverse domain wall motion along thin, narrow strips," J. Appl. Phys 95, pp. 6729-6731, June 2004.
24. L. Thomas, M. Hayashi, R. Moriya, C. Rettner, and S. Parkin, "Topological repulsion between domain walls in magnetic nanowires leading to the formation of bound states," Nature Communications (3) 810, May 2012.
25. N. L. Schryer, and L. R. Walker, "The motion of 180^{o} degree domain walls in uniform dc magnetic fields," *J. Appl. Phys*. **45** (12), pp. 5406-21, Apr.1974.
26. A. Kunz and J. Vogeler-Wunsch, "Application of local transverse fields for domain wall control in ferromagnetic nanowire arrays," Appl. Phys. Lett. 101, 192402 (2012).
27. A. Kunz and S. C. Reiff, "Dependence of domain wall structure for low field injection into magnetic nanowires," Appl. Phys. Lett. 94, 192504 (2009).
28. Y. Jang, S. R. Bowden, M. Mascaro, J. Unguris, and C. A. Ross, "Formation and structure of 360 and 540 degree domain walls in thin magnetic stripes," Appl. Phys. Lett. 100, 062407 (2012).

29. S.-M. Ahn, "Enhanced controllability of domain wall pinning by selective domain-wall injection," J. Appl. Phys. 113, 17B501 (2013).

Figures and Captions

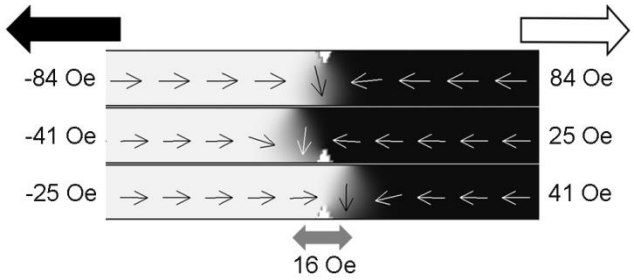

Fig. 1. Pinning locations and dynamic depinning fields for clockwise transverse domain walls. When the notch is located on the bottom edge of the wire the depinning field depends on the field direction. A 16 Oe fields can be used to transition the DW between the two pinning locations.

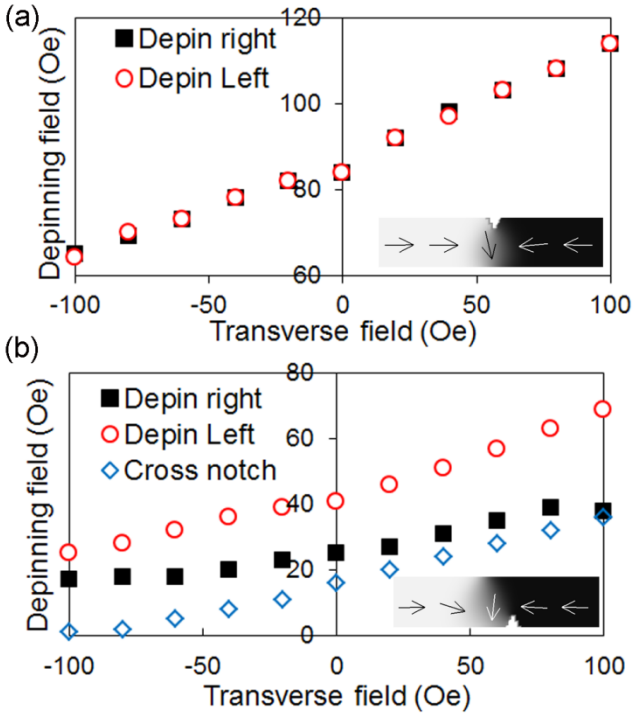

Fig. 2 The variation of the depinning field due to a transverse field applied parallel (-) or anti-parallel (+) to the magnetic moments in the domain wall. Parallel alignment lowers the depinning field. (b) The application of a weak field can be used to transition the DW between the two pinning locations on either side of the notch.

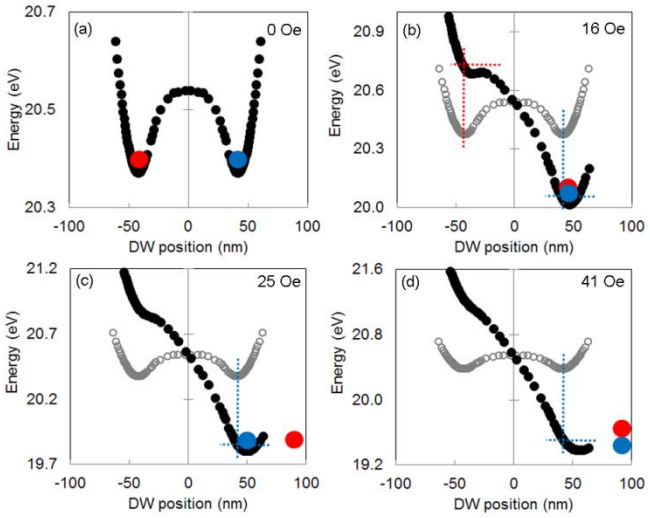

Fig. 3 The interaction potential for a trapped DW. The two minima in (a) correspond to the two trapping locations. A 16 Oe field (b) raises the DW (red dashed line) to an energy above the central maxima and the DW dynamically crosses the notch. 25 Oe (c) gives a DW in the left well enough KE to escape but the minima on the right still exists so a wall initially in the right well remains pinned. In (d) the DW is raised above the local maxima and the DW dynamically escapes.

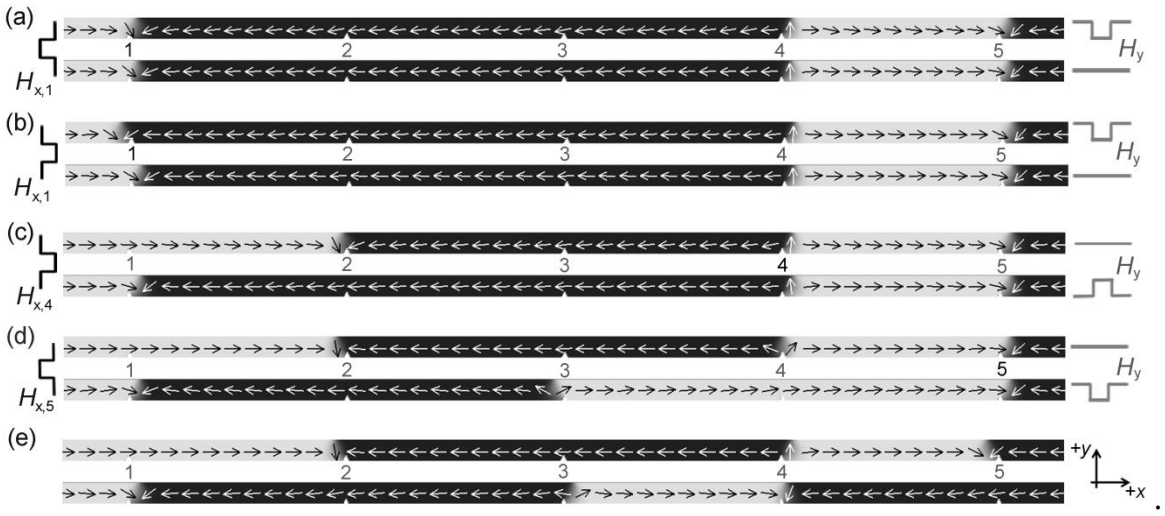

Fig. 4. Time dependent sequence of two wires each containing three DWs. (a) 10 Oe along the --x-axis at notch location 1 and 50 Oe along the –y-axis in the top wire transition the DW at notch 1 to that in (b). The series of pulses at the listed notch locations and in the wires shown move domain walls from notch location 1 to 2 in the top wire (c) , location 4 to 3 in the bottom wire (d), and finally location 5 to 4 in the bottom wire (e).